α-decay half-lives of superheavy nuclei

J. P. Cui (崔建坡),[1,2] Y. L. Zhang (张彦立),[1,2,3] S. Zhang (张闪),[1,2] and Y. Z. Wang (王艳召)[1,2,4,5,*]

[1]*Department of Mathematics and Physics, Shijiazhuang Tiedao University, Shijiazhuang 050043, China*
[2]*Institute of Applied Physics, Shijiazhuang Tiedao University, Shijiazhuang 050043, China*
[3]*Department of Physics, Beijing Jiaotong University, Beijing 10000, China*
[4]*China Institute of Atomic Energy, P.O. Box 275 (10), Beijing 102413, China*
[5]*Department of Nuclear Physics, KTH (Royal Institute of Technology), Alba Nova University Center, S-10691 Stockholm, Sweden*

The α-decay half-lives of superheavy nuclei (SHN) with $Z \geqslant 104$ are investigated by employing the effective liquid drop model (ELDM). By comparison between the calculated half-lives and the experimental ones, it is shown that the ELDM is a successful model to reproduce the experimental half-lives of SHN. Within the ELDM the α-decay half-lives of $Z = 118$–120 isotopes are predicted by inputting the α-decay energy (Q_α) values extracted from the newest Weizsäcker-Skyrme-4 (WS4) model, the finite-range droplet model (FRDM), the Kourra-Tachibaba-Uno-Yamada (KTUY) formula, and the Hartree-Fock-Bogoliubov mean field with the D1S Gogny force (GHFB). It is found that the shell effects at $N = 178$ and 184 are evident by analyzing the Q_α values and half-lives versus the neutron number N. Because the WS4 Q_α values have the smallest rms deviation, the predicted α-decay half-lives could be more accurate than the ones of other models, which will be helpful for future experiments.

I. INTRODUCTION

In recent years, study of superheavy nuclei (SHN) has become an interesting subject in modern nuclear physics [1–20]. With the development of detection technology and radioactive beam facilities, many superheavy elements or isotopes have been synthesized by cold, warm, and hot fusion reactions [3–20]. To date, nuclides with $Z \leqslant 118$ have been synthesized. For SHN, α decay is one of the most important decay modes, and it has yielded a powerful tool to identify new elements or new isotopes by detecting the α-decay chains [1–20]. In addition, via the observation of α decay one can obtain rich nuclear information, such as half-lives, released energies, radii, spin-parity, shell effects, and nuclear deformations [1–20].

α decay was firstly observed by Rutherford and Geiger at the beginning of the last century [21]. Subsequently, the α-decay phenomenon has been explained successfully as a quantum tunneling effect by Gamow [22] and by Condon and Gurney [23] in 1928. Since then, many phenomenological and microscopic models have been proposed to describe the α-decay process [24–58]. Among these models, the effective liquid drop model (ELDM) is a successful phenomenological model, which was proposed by Goncalves and Duarte in 1993 [58]. It is a superasymmetric fission model to study α decay, proton emission, cluster radioactivity, and clod fission in a unified framework. The experimental half-lives of these decay modes can be reproduced well by it [58–66]. About ten years ago, Zhang and Ren calculated α-decay half-lives of SHN within the ELDM [67]. They found that ELDM was a successful model

for reproducing experimental α-decay half-lives. However, in their work only the α-decay half-lives of even-even nuclei were calculated. In recent years, some new SHN have been synthesized and lots of newly experimental α-decay half-lives have been measured, which provide a foundation to test the predictive ability of the ELDM. So, it is necessary to extend the model to study the α-decay half-lives of more SHN. This is the motivation of this article. In fact, a successful model is very important. It is useful for searching for the magic numbers of the SHN region. In addition, the predicted half-lives where the experimental values are unavailable are helpful for experimental design. In this article we will extend the ELDM to calculate the α-decay half-lives of all synthesized SHN with $Z \geqslant 104$ and test its accuracy and predictive ability. This article is organized in the following way. In Sec. II the theoretical framework is introduced. The numerical results and corresponding discussions are given in Sec. III. In the last section, some conclusions are drawn.

II. ELDM

In ELDM, the system is considered as two spherical, molecular shape fragments of different radii in contact [58–62]. During the molecular phase of the process, the geometrical configuration of the deformed system is approximated by two intersecting spheres of different radii. As can be seen from Fig. 1, four independent coordinates (R_1, R_2, ζ, and ξ) are used to describe the dinuclear system.

In order to reduce the spherical four-dimensional problem to the equivalent one-dimensional one, three constraints are introduced. To keep the spherical segments in contact, it is

*yanzhaowang09@126.com
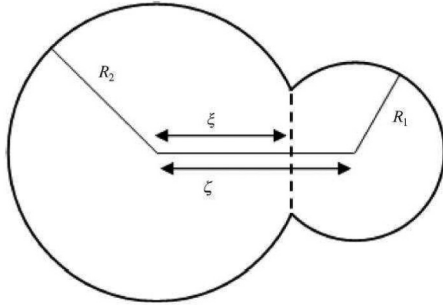
FIG. 1. Schematic representation of the dinuclear decaying system. R_1 and R_2 show the radii of the α particle and the daughter nucleus, respectively. ζ is the distance between their geometric centers. The variable ξ represents the distance between the plane of the intersection and the center of the daughter nucleus.

necessary to establish a geometric constraint,

$$R_1^2 - (\zeta - \xi)^2 = R_2^2 - \xi^2. \tag{1}$$

Considering the incompressibility of the nuclear matter, the constraint for conservation of total volume of the system is expressed by

$$2\left(R_1^3 + R_2^3\right) + 3\left[R_1^2(\zeta - \xi) + R_2^2\xi\right] - \left[(\zeta - \xi)^3 + \xi^3\right]$$
$$= 4R^3, \tag{2}$$

where R is the radius of the parent nucleus. Its value is determined by the simple formula

$$R = r_0 A^{1/3}. \tag{3}$$

Here r_0 is the most significant parameter used to make the model fit to the set of experimental data. A is the mass number of the parent nucleus.

In the varying mass asymmetry shape (VMAS) description, the radius of the α particle is regarded as constant, which is written as

$$R_1 - \overline{R}_1 = 0, \tag{4}$$

where $\overline{R}_1$ is the final radius of the α particle. It should be given by

$$\overline{R}_i = \left(\frac{Z_i}{Z}\right)^{1/3} R \quad (i = 1, 2), \tag{5}$$

where Z, Z_1, and Z_2 are the charge numbers of the parent nucleus, emitted particle, and daughter nucleus, respectively. Then the α decay is conveniently reduced to the effective one-dimensional potential barrier penetrability problem. In order to evaluate the half-life of a given parent nucleus, the Gamow penetrability factor should be calculated by

$$P = \exp\left[-\frac{2}{\hbar} \int_{\zeta_0}^{\zeta_c} \sqrt{2\mu_{WW}^{VMAS}[V(\zeta) - Q_\alpha]} \, d\zeta\right]. \tag{6}$$

Here, the limits ζ_0 and ζ_c of the integral are the inner and outer turning points, respectively. $V(\zeta)$ is the one-dimensional total potential energy which consists of Coulomb energy, effective surface energy, and the centrifugal potential energy [58]. μ_{WW}^{VMAS} is the inertial coefficient obtained by making use

of the Werner-Wheeler approximation [68] for the velocity field of the nuclear flow within the VMAS description.

Finally, the α-decay half-life is calculated as

$$T_{1/2}(s) = \frac{\ln 2}{\nu_0 P}, \tag{7}$$

where ν_0 is the frequency of assaults on the barrier, whose value is determined in order to obtain the best agreement with experimental data. For calculations on α-decay half-lives, ν_0 and r_0 are taken as 1.8×10^{22} s^{-1} and 1.34 fm, respectively [62].

III. RESULTS AND DISCUSSIONS

The α-decay half-lives of SHN with $Z \geqslant 104$ have been calculated by inputting the experimental Q_α values within the ELDM. Note that in the calculations the orbital angular momenta carried by α particles are selected as 0 because the spin-parities of SHN are unknown. The detailed results of 80 known SHN are listed in Table I. In Table I the first column indicates the parent nuclei. The second column gives the experimental Q_α values. The experimental data and the calculated half-lives are listed in columns 3 and 4, respectively. In order to test the agreement between the experimental half-lives and the calculated ones, the average deviation $\overline{\sigma}$ and the standard deviation $\sqrt{\overline{\sigma^2}}$ are usually calculated by the following expressions:

$$\overline{\sigma} = \frac{1}{n} \sum_{i=1}^{n} \left| \log_{10} T_{1/2}^{\text{expt.}\,i} - \log_{10} T_{1/2}^{\text{calc.}\,i} \right|, \tag{8}$$

$$\sqrt{\overline{\sigma^2}} = \left[\frac{1}{n} \sum_{i=1}^{n} \left(\log_{10} T_{1/2}^{\text{expt.}\,i} - \log_{10} T_{1/2}^{\text{calc.}\,i}\right)^2\right]^{1/2}. \tag{9}$$

By using Eqs. (8) and (9) the $\overline{\sigma}$ and $\sqrt{\overline{\sigma^2}}$ can be obtained; their values are 0.54 and 0.58, respectively. This means that the average deviation between the experimental half-lives and the calculated ones is within a factor of 3.80, which indicates that the α-decay half-lives of SHN can be reproduced well by ELDM.

In addition, the hindrance factor (HF) is usually applied to analyze the deviation between the experimental half-lives and the theoretical ones; it is expressed as

$$\text{HF} = T_{1/2}^{\text{expt.}} / T_{1/2}^{\text{calc.}}. \tag{10}$$

The values of HF are listed in the last column of Table I. Usually one defines that if the HF value is within a factor of 10, the theoretical results will be in agreement with the experimental data. In Table I, good agreements between the experimental half-lives and the calculated ones are found except in the cases of $^{258}105$, $^{260}107$, $^{279}111$, and $^{281}111$. We think the deviations are probably occurring for the following reasons. First, $^{258}105$ and $^{260}107$ are odd-odd nuclei. The formation of α-particles will be more difficult because of the odd nucleon blocking effect. However, the ELDM is a phenomenological model and the blocking effect is not included, so that the α-decay half-lives of the two nuclei will be underestimated. For $^{279}111$ and $^{281}111$, the large deviations

TABLE I. The experimental and calculated α-decay half-lives of SHN with $Z \geqslant 104$. The experimental half-lives and Q_α values are taken from Refs. [3–18,69–71].

Nucleus	Q_α (MeV)	$T_{1/2}^{\text{expt.}}$ (s)	$T_{1/2}^{\text{ELDM}}$ (s)	HF
^{255}104	9.05 [69]	4.42×10^0 [69]	1.18×10^0	3.75
^{256}104	8.93 [70]	2.08×10^0 [71]	2.81×10^0	0.74
^{258}104	9.19 [70]	1.06×10^{-1} [71]	4.20×10^{-1}	0.25
^{259}104	9.13 [69]	2.60×10^0 [69]	6.09×10^{-1}	4.28
^{261}104	8.65 [70]	8.15×10^0 [71]	1.75×10^1	0.47
^{263}104	8.25 [69]	2.00×10^3 [69]	3.59×10^2	5.57
^{256}105	9.34 [70]	2.84×10^0 [71]	3.82×10^{-1}	7.43
^{257}105	9.21 [69]	2.45×10^0 [69]	9.08×10^{-1}	2.69
^{258}105	9.50 [69]	5.58×10^0 [69]	1.24×10^{-1}	45.10
^{259}105	9.62 [70]	5.10×10^{-1} [71]	5.52×10^{-2}	9.24
^{270}105	8.02 [3]	3.60×10^3 [3]	4.72×10^3	0.76
^{259}106	9.80 [70]	3.11×10^{-1} [71]	3.90×10^{-2}	7.98
^{260}106	9.90 [70]	1.24×10^{-2} [71]	2.06×10^{-2}	0.60
^{261}106	9.71 [70]	1.87×10^{-1} [71]	6.38×10^{-2}	2.93
^{263}106	9.40 [70]	1.08×10^0 [71]	4.56×10^{-1}	2.37
^{267}106	8.32 [4]	6.35×10^2 [4]	1.06×10^3	0.60
^{269}106	8.70 [70]	4.80×10^2 [71]	5.27×10^1	9.11
^{271}106	8.66 [5]	1.63×10^2 [5]	6.25×10^1	2.61
^{260}107	10.4 [69]	3.50×10^{-2} [69]	2.35×10^{-3}	14.89
^{261}107	10.5 [69]	1.18×10^{-2} [69]	1.28×10^{-3}	9.22
^{265}107	9.38 [6]	9.40×10^{-1} [6]	1.11×10^0	0.85
^{266}107	9.43 [7]	2.50×10^0 [7]	7.60×10^{-1}	3.29
^{267}107	8.96 [7]	2.20×10^1 [7]	1.91×10^1	1.15
^{270}107	9.06 [69]	6.00×10^1 [69]	8.63×10^0	6.95
^{272}107	9.14 [8]	8.18×10^0 [8]	4.43×10^0	1.84
^{274}107	8.97 [3]	3.00×10^1 [3]	1.43×10^1	2.09
^{264}108	10.59 [69]	1.60×10^{-3} [69]	1.48×10^{-3}	1.08
^{265}108	10.47 [70]	1.96×10^{-3} [71]	2.82×10^{-3}	0.69
^{266}108	10.35 [69]	2.30×10^{-3} [69]	5.58×10^{-3}	0.41
^{268}108	9.62 [70]	1.42×10^0 [71]	4.55×10^{-1}	3.12
^{269}108	9.32 [9]	1.52×10^1 [9]	3.39×10^0	4.48
^{270}108	9.15 [10]	7.60×10^0 [10]	1.07×10^1	0.71
^{273}108	9.73 [70]	9.10×10^{-1} [71]	1.90×10^{-1}	4.79
^{275}108	9.44 [70]	2.90×10^{-1} [71]	1.20×10^0	0.24
^{270}109	10.18 [70]	6.30×10^{-3} [71]	2.83×10^{-2}	0.22
^{274}109	10.04 [11]	4.44×10^{-1} [11]	5.90×10^{-2}	7.53
^{275}109	10.48 [12]	9.70×10^{-3} [12]	3.99×10^{-3}	2.43
^{276}109	9.81 [69]	7.20×10^{-1} [69]	2.27×10^{-1}	3.17
^{278}109	9.59 [3]	3.60×10^0 [3]	9.03×10^{-1}	3.98
^{267}110	11.78 [70]	1.00×10^{-5} [71]	1.71×10^{-5}	0.85
^{269}110	11.51 [69]	1.79×10^{-4} [69]	4.13×10^{-5}	4.33
^{270}110	11.12 [70]	2.05×10^{-4} [71]	3.00×10^{-4}	0.68
^{271}110	10.87 [69]	1.63×10^{-3} [69]	1.10×10^{-3}	1.48
^{273}110	11.37 [69]	1.70×10^{-4} [69]	7.25×10^{-5}	2.34
^{277}110	10.83 [69]	4.10×10^{-3} [69]	1.11×10^{-3}	3.69
^{279}110	9.84 [5]	2.00×10^0 [5]	3.82×10^{-1}	5.23
^{281}110	8.86 [13]	2.22×10^2 [13]	3.55×10^2	0.63
^{272}111	11.20 [69]	3.80×10^{-3} [69]	3.81×10^{-4}	9.97
^{278}111	10.85 [69]	4.20×10^{-3} [69]	2.03×10^{-3}	2.07
^{279}111	10.52 [69]	1.70×10^{-1} [69]	1.29×10^{-2}	13.18
^{280}111	9.89 [8]	3.53×10^0 [8]	5.96×10^{-1}	5.94
^{281}111	9.41 [14]	1.70×10^2 [14]	1.42×10^1	11.97
^{282}111	9.08 [3]	1.86×10^2 [3]	1.47×10^2	1.26
^{277}112	11.62 [69]	6.90×10^{-4} [69]	7.42×10^{-5}	9.29
^{281}112	10.46 [69]	1.3×10^{-1} [69]	3.70×10^{-2}	3.51

TABLE I. *(Continued.)*

Nucleus	Q_α (MeV)	$T_{1/2}^{\text{expt.}}$ (s)	$T_{1/2}^{\text{ELDM}}$ (s)	HF
^{283}112	9.67 [15]	3.80×10^0 [15]	5.21×10^0	0.73
^{284}112	9.30 [16]	9.81×10^0 [16]	6.61×10^1	0.15
^{285}112	9.32 [70]	3.20×10^1 [71]	5.57×10^1	0.57
^{278}113	11.85 [69]	2.40×10^{-4} [69]	4.61×10^{-5}	5.20
^{282}113	10.78 [69]	7.00×10^{-2} [69]	1.18×10^{-2}	5.92
^{283}113	10.26 [12]	1.02×10^{-1} [12]	2.47×10^{-1}	0.41
^{284}113	10.11 [8]	9.43×10^{-1} [8]	6.22×10^{-1}	1.51
^{285}113	9.84 [8]	3.22×10^0 [8]	3.52×10^0	0.91
^{286}113	9.79 [69]	2.00×10^1 [69]	4.75×10^0	4.21
^{285}114	10.54 [17]	4.70×10^{-1} [17]	9.36×10^{-2}	5.02
^{286}114	10.37 [70]	3.50×10^{-1} [71]	2.54×10^{-1}	1.38
^{287}114	10.16 [70]	5.20×10^{-1} [71]	9.15×10^{-1}	0.57
^{288}114	10.07 [70]	7.50×10^{-1} [71]	1.55×10^0	0.48
^{289}114	9.97 [70]	2.40×10^0 [71]	2.91×10^0	0.82
^{287}115	10.74 [70]	1.20×10^{-1} [71]	5.71×10^{-2}	2.10
^{288}115	10.63 [70]	1.90×10^{-1} [71]	1.06×10^{-1}	1.79
^{289}115	10.49 [8]	2.00×10^{-1} [8]	2.40×10^{-1}	0.83
^{290}115	10.45 [3]	1.30×10^0 [3]	2.95×10^{-1}	4.41
^{290}116	10.99 [70]	8.00×10^{-3} [71]	2.57×10^{-2}	0.31
^{291}116	10.89 [70]	2.80×10^{-2} [71]	4.41×10^{-2}	0.64
^{292}116	10.77 [70]	2.40×10^{-2} [71]	8.41×10^{-2}	0.29
^{293}116	10.68 [70]	8.00×10^{-2} [71]	1.42×10^{-1}	0.56
^{293}117	11.18 [18]	1.46×10^{-2} [18]	1.66×10^{-2}	0.88
^{294}117	11.20 [3]	5.10×10^{-2} [3]	1.43×10^{-2}	3.57
^{294}118	11.81 [70]	1.40×10^{-3} [71]	1.10×10^{-3}	1.28

between the calculated half-lives and the experimental ones are also from the blocking effect because they are odd-A nuclei. In addition, in our calculations the orbital angular momenta carried by α particles are selected as 0. Usually, the orbital angular momenta carried by α particles are not 0 for the odd-odd and odd-A nuclei. Thus the calculated half-lives will be decreased slightly. If the orbital angular momenta are taken into account in the calculations, the computed half-lives will be closer to the experimental data. Nevertheless, as a whole the ELDM is a successful model for studying α decay of SHN. Encouraged by the agreement mentioned above, we will attempt to predict with the ELDM the α-decay half-lives of SHN where the experimental data are not available.

In calculations of α-decay half-lives, we know that the Q_α values play a crucial role. Usually the Q_α values can be derived by the relationship between the Q_α value and the nuclear mass excess M:

$$Q_\alpha(Z,N) = M(Z,N) - M(Z-2, N-2) - M(2,2). \quad (11)$$

To get the accurate Q_α values of SHN, a reliable mass model is very necessary. In recent years, many nuclear mass models with different accuracy have been developed [72–79]. In the present work, we select four kinds of mass models to get the Q_α values: they are the WS4 [76], the FRDM [77], the KTUY [78], and the GHFB [79] models, respectively. Then the α-decay half-lives of $Z = 118$–120 isotopes are calculated within the ELDM by inputting the Q_α values extracted from the above mentioned four kinds of nuclear mass tables. The Q_α values of four kinds of mass tables and corresponding half-lives of $Z = 118$–120 isotopes are listed in Table II. From Table II, we

TABLE II. The predicted $\log_{10} T_{1/2}$ values of $Z = 118$–120 isotopes by inputting the Q_α values extracted from the WS4, FRDM, KTUY, and GHFB mass tables. The Q_α values and the α-decay half-lives are measured in MeV and seconds, respectively. The symbol * denotes the experimental values of $^{294}118$.

Nucleus	Q_α^{WS4}	Q_α^{FRDM}	Q_α^{KTUY}	Q_α^{GHFB}	$\log_{10} T_{1/2}^{\text{WS4}}$	$\log_{10} T_{1/2}^{\text{FRDM}}$	$\log_{10} T_{1/2}^{\text{KTUY}}$	$\log_{10} T_{1/2}^{\text{GHFB}}$
$^{289}118$	12.59	12.76	11.79	12.32	−4.56	−4.89	−2.83	−4.00
$^{290}118$	12.60	12.67	11.65	12.22	−4.59	−4.72	−2.52	−3.80
$^{291}118$	12.42	12.55	11.60	10.90	−4.24	−4.49	−2.42	−0.73
$^{292}118$	12.24	12.39	11.47	10.58	−3.87	−4.18	−2.13	0.10
$^{293}118$	12.24	12.34	11.28	11.44	−3.89	−4.09	−1.69	−2.09
$^{294}118$	11.81*				−2.85*			
$^{295}118$	11.90	11.93	11.11	10.23	−3.18	−3.23	−1.30	1.02
$^{296}118$	11.75	12.28	10.95	10.15	−2.86	−4.01	−0.92	1.24
$^{297}118$	12.10	12.39	11.02	11.01	−3.65	−4.25	−1.11	−1.10
$^{298}118$	12.18	12.49	11.12	10.85	−3.84	−4.47	−1.37	−0.70
$^{299}118$	12.05	12.51	11.04	10.08	−3.56	−4.53	−1.19	1.40
$^{300}118$	11.96	12.51	11.04	10.17	−3.37	−4.54	−1.20	1.12
$^{301}118$	12.02	12.56	11.03	10.06	−3.53	−4.66	−1.19	1.42
$^{302}118$	12.04	12.62	10.92	10.02	−3.59	−4.79	−0.93	1.53
$^{303}118$	12.60	13.38	11.70	11.84	−4.79	−6.27	−2.83	−3.16
$^{304}118$	13.12	13.40	12.44	12.32	−5.82	−6.32	−4.45	−4.21
$^{290}119$	13.07	13.31	12.31	12.92	−5.23	−5.68	−3.68	−4.94
$^{291}119$	13.05	13.24	12.17	12.78	−5.20	−5.56	−3.40	−4.68
$^{292}119$	12.90	13.08	12.10	11.33	−4.93	−5.27	−3.26	−1.49
$^{293}119$	12.72	12.92	11.99	10.99	−4.58	−4.97	−3.03	−0.66
$^{294}119$	12.73	12.85	11.85	11.88	−4.61	−4.85	−2.73	−2.81
$^{295}119$	12.76	12.94	11.71	11.21	−4.69	−5.04	−2.43	−1.24
$^{296}119$	12.48	12.98	11.51	10.62	−4.13	−5.14	−1.97	0.27
$^{297}119$	12.42	12.90	11.29	10.50	−4.04	−4.99	−1.46	0.58
$^{298}119$	12.71	13.09	11.33	11.41	−4.65	−5.38	−1.57	−1.78
$^{299}119$	12.76	13.08	11.48	11.24	−4.76	−5.37	−1.95	−1.38
$^{300}119$	12.57	13.03	11.40	10.44	−4.39	−5.29	−1.77	0.70
$^{301}119$	12.43	13.08	11.35	10.51	−4.10	−5.40	−1.66	0.49
$^{302}119$	12.43	13.05	11.31	10.60	−4.11	−5.36	−1.58	0.23
$^{303}119$	12.42	13.11	11.22	10.53	−4.11	−5.49	−1.37	0.41
$^{304}119$	12.93	13.86	12.03	12.27	−5.16	−6.87	−3.28	−3.81
$^{305}119$	13.42	13.86	12.82	12.72	−6.12	−6.89	−4.95	−4.76
$^{291}120$	13.51	13.87	12.82	12.53	−5.79	−6.44	−4.46	−3.88
$^{292}120$	13.47	13.78	12.72	12.35	−5.73	−6.29	−4.27	−3.51
$^{293}120$	13.40	13.65	12.57	10.85	−5.62	−6.07	−3.98	0.03
$^{294}120$	13.24	13.49	12.50	10.57	−5.34	−5.80	−3.85	0.77
$^{295}120$	13.27	13.46	12.36	11.42	−5.41	−5.75	−3.57	−1.44
$^{296}120$	13.34	13.59	12.23	11.36	−5.56	−6.01	−3.30	−1.31
$^{297}120$	13.14	13.65	11.98	11.06	−5.19	−6.13	−2.76	−0.57
$^{298}120$	13.01	13.24	11.63	11.26	−4.94	−5.38	−1.97	−1.09
$^{299}120$	13.26	13.73	11.67	11.89	−5.44	−6.30	−2.08	−2.6
$^{300}120$	13.32	13.70	11.89	11.72	−5.57	−6.26	−2.60	−2.22
$^{301}120$	13.06	13.62	11.84	10.88	−5.10	−6.13	−2.50	−0.16
$^{302}120$	12.89	13.55	11.80	11.12	−4.77	−6.02	−2.43	−0.80
$^{303}120$	12.81	13.51	11.69	10.96	−4.63	−5.96	−2.19	−0.40
$^{304}120$	12.76	13.55	11.52	10.88	−4.54	−6.05	−1.80	−0.21
$^{305}120$	13.28	14.26	12.39	12.74	−5.57	−7.31	−3.78	−4.51
$^{306}120$	13.79	14.28	13.23	13.18	−6.51	−7.36	−5.48	−5.39

can see that for the same isotopic chains the extracted Q_α values are different. This indicates that the Q_α values are dependent strongly on the mass models. Because the α-decay half-lives are very sensitive to the Q_α values, the predicted half-lives are different largely due to inputting different Q_α values. We know that the search for the magic numbers of the SHN has

been an interesting subject in modern nuclear physics. To get information on the magic numbers, the extracted Q_α values and the predicted $\log_{10} T_{1/2}$ as functions of N are plotted in Fig. 2. According to Fig. 2, the shell effects at $N = 178$ and $N = 184$ are evident for all the cases. In other words, although the calculated Q_α and half-life values are model dependent, the
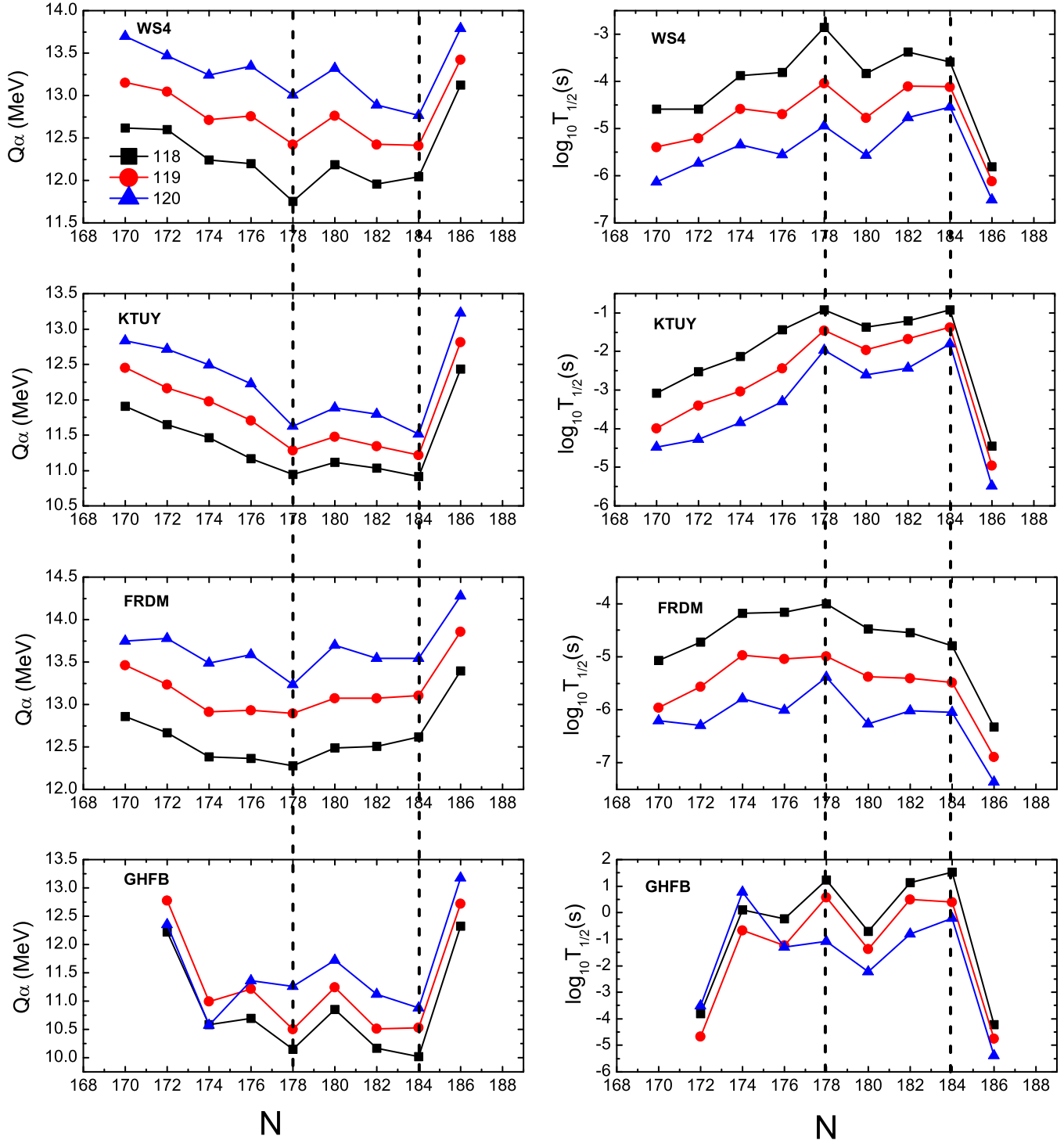
FIG. 2. Left column: The extracted Q_α values of $Z = 118$–120 isotopes versus N for four kinds of mass tables. Right column: The corresponding $\log_{10}T_{1/2}$ values of $Z = 118$–120 isotopes versus N with ELDM. The vertical dashed lines represent the magic numbers at $N = 178, 184$ of parent nuclei.

predicted magic numbers are the same. To date, the heaviest synthesized nucleus is $^{294}118$ with $N = 176$. From Fig. 2 we know that the half-life of $^{296}118$ is longer than that of $^{294}118$ because of the shell effect at $N = 178$. So $^{296}118$ is synthesized more easily than $^{294}118$, a finding to which attention should be paid by experimental researchers.

Finally, we will discuss the accuracies of the four kinds of α-decay half-lives in Table II. In the preceding paragraph, we mentioned that the α-decay half-lives are dependent strongly on the Q_α accuracies. By taking the $Z = 120$ isotopes as an example, the Q_α and $\log_{10}T_{1/2}$ values versus N for four kinds of mass models are shown in Fig. 3. From Fig. 3, one can
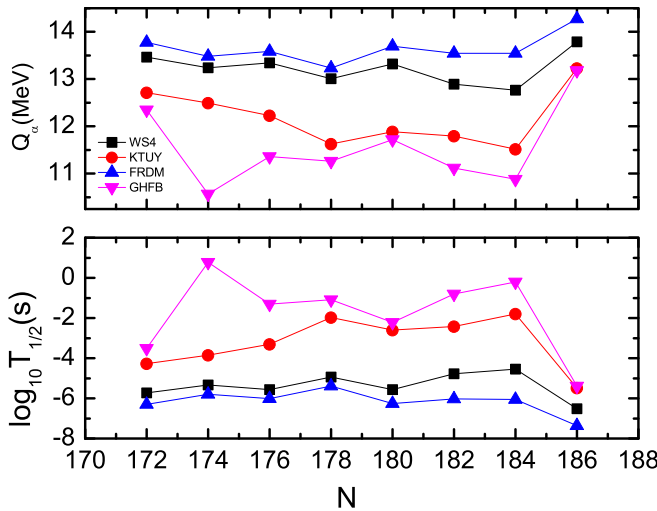
FIG. 3. The Q_α values of four kinds of mass tables (top) and the corresponding $\log_{10} T_{1/2}$ values (bottom) of $Z = 120$ isotopes as functions of N.

see that for $^{294}120$ the 2.70 MeV uncertainty of Q_α results in 10^6 times uncertainty of the α-decay half-lives. Corresponding study suggests that the WS4 rms deviation with respect to the 2353 known masses falls to 0.298 MeV [76]. Moreover, recent studies [24,80] indicate that the WS4 mass model is more accurate than the other mass models by systematic analysis. So we believe the α-decay half-lives of column 6 are more accurate, and are useful for future experiments.

IV. CONCLUSIONS

In this article, the α-decay half-lives of SHN with $Z \geqslant 104$ have been investigated by the ELDM. By comparisons between the calculated half-lives and the experimental data, it is found that the experimental half-lives of the SHN can be reproduced well within the ELDM. In addition, the ELDM has been used to predict the α-decay half-lives that are unmeasured by inputting four kinds of Q_α values, which are extracted from the WS4, FRDM, GHFB, and KTUY mass tables. By systematic analysis, it is shown that the shell effects at $N = 178$ and $N = 184$ are evident for all the cases. Meanwhile, it is found that the superheavy nuclide $^{296}118$ will be synthesized more easily than $^{294}118$ because of the shell effect at $N = 178$, a finding to which attention should be paid attention by researchers. Last, we know that the predicted half-lives by inputting the WS4 Q_α values are the most accuracy ones, and are helpful for future experiments.

[1] S. Hofmann, Rep. Prog. Phys. **61**, 639 (1998).

[2] J. H. Hamilton, S. Hofmann, and Y. T. Oganessian, Annu. Rev. Nucl. Part. Sci. **63**, 383 (2013).

[3] J. Khuyagbaatar, A. Yakushev, Ch. E. Düllmann *et al.*, Phys. Rev. Lett. **112**, 172501 (2014).

[4] J. Dvorak, W. Brüchle, M. Chelnokov *et al.*, Phys. Rev. Lett. **100**, 132503 (2008).

[5] Yu. Ts. Oganessian, V. K. Utyonkov, Yu. V. Lobanov *et al.*, Phys. Rev. C **74**, 044602 (2006).

[6] Z. G. Gan, J. S. Guo, X. L. Wu *et al.*, Eur. Phys. J. A **20**, 385 (2004).

[7] P. A. Wilk, K. E. Gregorich, A. Türler *et al.*, Phys. Rev. Lett. **85**, 2697 (2000).

[8] Yu. Ts. Oganessian, F. Sh. Abdullin, S. N. Dmitriev *et al.*, Phys. Rev. Lett. **108**, 022502 (2012).

[9] S. Hofmann and G. Münzenberg, Rev. Mod. Phys. **72**, 733 (2000).

[10] Yu. Oganessian, Radiochim. Acta **99**, 429 (2011).

[11] Yu. Ts. Oganessian, V. K. Utyonkov, Yu. V. Lobanov *et al.*, Phys. Rev. C **76**, 011601 (2007).

[12] Yu. Ts. Oganessian, V. K. Utyonkoy, Yu. V. Lobanov *et al.*, Phys. Rev. C **69**, 021601(R) (2004).

[13] Ch. E. Düllmann, M. Schädel, A. Yakushev *et al.*, Phys. Rev. Lett. **104**, 252701 (2010).

[14] Yu. Ts. Oganessian, F. Sh. Abdullin, C. Alexander *et al.*, Phys. Rev. C **87**, 054621 (2013).

[15] Yu. Oganessian, J. Phys. G: Nucl. Part. Phys. **34**, R165 (2007).

[16] Yu. Ts. Oganessian, V. K. Utyonkov, Yu. V. Lobanov *et al.*, Phys. Rev. C **62**, 041604 (2000).

[17] P. A. Ellison, K. E. Gregorich, J. S. Berryman *et al.*, Phys. Rev. Lett. **105**, 182701 (2010).

[18] Yu. Ts. Oganessian, F. Sh. Abdullin, P. D. Bailey *et al.*, Phys. Rev. Lett. **104**, 142502 (2010).

[19] K. Morita, K. Morimoto, D. Kaji *et al.*, J. Phys. Soc. Jpn. **73**, 2593 (2004); **81**, 103201 (2012).

[20] Z. Y. Zhang, Z. G. Gan, L. Ma *et al.*, Chin. Phys. Lett. **29**, 012502 (2012).

[21] E. Rutherfold and H. Geiger, Proc. R. Soc. London A **81**, 162 (1908).

[22] G. Gamow, Z. Phys. **51**, 204 (1928).

[23] E. U. Condon and R. W. Gurney, Nature (London) **122**, 439 (1928).

[24] Y. Z. Wang, S. J. Wang, Z. Y. Hou, and J. Z. Gu, Phys. Rev. C **92**, 064301 (2015).

[25] D. S. Delion and A. Sandulescu, J. Phys. G: Nucl. Part. Phys. **28**, 617 (2002).

[26] H. F. Zhang, G. Royer, Y. J. Wang, J. M. Dong, W. Zuo, and J. Q. Li, Phys. Rev. C **80**, 057301 (2009).

[27] K. P. Santhosh, S. Sabina, and R. K. Biju, Nucl. Phys. A **825**, 159 (2009).

[28] A. Sobiczewski and A. Parkhomenko, Prog. Part. Nucl. Phys. **58**, 292 (2007).

[29] D. N. Poenaru, R. A. Gherghescu, and N. Carjan, Europhys. Lett. **77**, 62001 (2007).

[30] V. Yu. Denisov and A. A. Khudenko, Phys. Rev. C **79**, 054614 (2009).

[31] R. G. Lovas, R. J. Liotta, K. Varga, and D. S. Delion, Phys. Rep. **294**, 265 (1998).

[32] P. E. Hodgson and E. Bétäk, Phys. Rep. **374**, 1 (2003).

[33] B. Buck, A. C. Merchant, and S. M. Perez, At. Data Nucl. Data Tables **54**, 53 (1993).

[34] J. Wauters, P. Dendooven, M. Huyse, G. Reusen, P. Van Duppen, and P. Lievens (The ISOLDE Collaboration), Phys. Rev. C **47**, 1447 (1993).

[35] G. Royer, J. Phys. G: Nucl. Part. Phys. **26**, 1149 (2000).

[36] N. D. Schubert and M. A. Reyes, At. Data Nucl. Data Tables **93**, 907 (2007).

[37] N. D. Schubert, M. A. Reyes, and V. A. Tamez, Eur. Phys. J. A **42**, 121 (2009).

[38] R. Moustabchir and G. Royer, Nucl. Phys. A **683**, 266 (2001).

[39] P. Mohr, Eur. Phys. J. A **31**, 23 (2007).

[40] L. L. Li, S. G. Zhou, E. G. Zhao, and W. Scheid, Int. J. Mod. Phys. E **19**, 359 (2010).

[41] W. H. Long, J. Meng, and S. G. Zhou, Phys. Rev. C **65**, 047306 (2002).

[42] S. Zhang, Y. L. Zhang, J. P. Cui, and Y. Z. Wang, Phys. Rev. C **95**, 014311 (2017).

[43] Y. L. Zhang and Y. Z. Wang, Nucl. Phys. A **966**, 102 (2017).

[44] J. P. Cui, Y. L. Zhang, S. Zhang, and Y. Z. Wang, Int. J. Mod. Phys. E **25**, 1650056 (2016).

[45] V. E. Viola, Jr. and G. T. Seaborg, J. Inorg. Nucl. Chem. **28**, 741 (1966).

[46] D. N. Poenaru, M. Ivascu, and D. Mazilu, Comput. Phys. Commun. **25**, 297 (1982).

[47] D. N. Poenaru and W. Greiner, Phys. Scr. **44**, 427 (1991).

[48] D. N. Poenaru, *Nuclear Decay Modes* (Institute of Physics, Bristol, 1996).

[49] A. Parkhomenko and A. Sobiczewski, Acta Phys. Pol. B **36**, 1363 (2005).

[50] D. Ni, Z. Ren, T. Dong, and C. Xu, Phys. Rev. C **78**, 044310 (2008).

[51] D. N. Poenaru, R. A. Gherghescu, and W. Greiner, Phys. Rev. C **83**, 014601 (2011).

[52] D. N. Poenaru, R. A. Gherghescu, and W. Greiner, Phys. Rev. C **85**, 034615 (2012).

[53] C. Qi, F. R. Xu, R. J. Liotta, and R. Wyss, Phys. Rev. Lett. **103**, 072501 (2009).

[54] D. N. Poenaru, D. Schnabel, W. Greiner *et al.*, At. Data Nucl. Data Tables **48**, 231 (1991).

[55] D. N. Poenaru and W. Greiner, *Clusters in Nuclei*, Lecture Notes in Physics Vol. 818, edited by by C. Beck (Springer, Berlin, 2010), Vol. 1, Chap. 1.

[56] D. N. Poenaru, R. A. Gherghescu, and W. Greiner, Phys. Rev. Lett. **107**, 062503 (2011).

[57] D. T. Akrawy and D. N. Poenaru, J. Phys. G: Nucl. Part. Phys. **44**, 105105 (2017).

[58] M. Goncalves and S. B. Duarte, Phys. Rev. C **48**, 2409 (1993).

[59] M. Goncalves, S. B. Duarte, F. Garcia, and O. Rodriguez, Comput. Phys. Commun. **107**, 246 (1997).

[60] O. A. P. Tavares, S. B. Duarte, O. Rodríguez *et al.*, J. Phys. G: Nucl. Part. Phys. **24**, 1757 (1998).

[61] S. B. Duarte, O. Rodriguez, O. A. P. Tavares, M. Gonçalves, F. García, and F. Guzmán, Phys. Rev. C **57**, 2516 (1998).

[62] S. B. Duarte, O. A. P. Tavares, F. Guzman, and A. Dimarco, At. Data Nucl. Data Tables **80**, 235 (2002).

[63] Y. Z. Wang, Z. Y. Li, G. L. Yu, and Z. Y. Hou, J. Phys. G: Nucl. Part. Phys. **41**, 055102 (2014).

[64] X. P. Zhang and Z. Z. Ren, J. Phys. G: Nucl. Part. Phys. **31**, 959 (2005).

[65] Y. Z. Wang, J. P. Cui, Y. L. Zhang, S. Zhang, and J. Z. Gu, Phys. Rev. C **95**, 014302 (2017).

[66] Z. Q. Sheng, L. P. Shu, G. W. Fan *et al.*, Chin. Phys. C **39**, 024102 (2015).

[67] X. P. Zhang and Z. Z. Ren, High Energy Phys. Nucl. Phys. **30**, 47 (2006) (in Chinese).

[68] D. N. Poenaru, J. A. Maruhn, W. Greiner *et al.*, Z. Phys. A **333**, 291 (1989).

[69] NuDat2.7, http://www.nndc.bnl.gov.

[70] M. Wang, G. Audi, F. G. Kondev, W. J. Huang, S. Naimi, and X. Xu, Chin. Phys. C **41**, 030003 (2017).

[71] G. Audi, F. G. Kondev, M. Wang, W. J. Huang, and S. Naimi, Chin. Phys. C **41**, 030001 (2017).

[72] G. Royer and A. Subercaze, Nucl. Phys. A **917**, 1 (2013).

[73] A. Bhagwat, Phys. Rev. C **90**, 064306 (2014).

[74] X. Y. Qu, Y. Chen, S. Q. Zhang *et al.*, Sci. China Phys. Mech. Astron. **56**, 2031 (2013).

[75] C. Qi, J. Phys. G: Nucl. Part. Phys. **42**, 045104 (2015).

[76] N. Wang, M. Liu, X. Z. Wu, and J. Meng, Phys. Lett. B **734**, 215 (2014); http://www.imqmd.com/mass/.

[77] P. Möller, A. J. Sierk, T. Ichikawa, and H. Sagawa, At. Data Nucl. Data Tables **109-110**, 1 (2016).

[78] H. Koura, T. Tachibana, and M. Uno, Prog. Theor. Phys. **113**, 305 (2005).

[79] http://www-phynu.cea.fr/science_en_ligne/carte_potentiels_microscopiques/carte_potentiel_nucleaire.htm.

[80] Z. Y. Wang, Z. M. Niu, Q. Liu, and J. Y. Guo, J. Phys. G: Nucl. Part. Phys. **42**, 055112 (2015).